Molecular Pharmacology Fast Forward. Published on December 9, 2004 as doi:10.1124/mol.104.002931
This article has not been copyedited and formatted. The final version may differ from this version.

Tyr702 is an Important Determinant of Agonist Binding and Domain Closure of the Ligand-Binding Core of GluR2

Anne Frandsen, Darryl S. Pickering, Bente Vestergaard, Christina Kasper, Bettina Bryde Nielsen, Jeremy R. Greenwood, Giuseppe Campiani, Caterina Fattorusso, Michael Gajhede, Arne Schousboe and Jette Sandholm Kastrup

Biostructural Research, Department of Medicinal Chemistry (A.F., B.V., C.K., B.B.N., J.R.G., M.G., J.S.K.) and Department of Pharmacology (D.S.P., A.S.), Danish University of Pharmaceutical Sciences, Universitetsparken 2, DK-2100 Copenhagen, Denmark; Dipartimento Farmaco Chimico Tecnologico, Via Aldo Moro, and European Research Centre for Drug Discovery and Development, Siena University, Siena 53100, Italy (G.C.); Dipartimento di Chimica delle Sostanze Naturali, Napoli University, via D. Montesano, 80131 Napoli, Italy (C.F.)

Molecular Pharmacology Fast Forward. Published on December 9, 2004 as DOI: 10.1124/mol.104.002931
This article has not been copyedited and formatted. The final version may differ from this version.

Running title: Role of Y702 in agonist binding and domain closure of GluR2

Corresponding author: Jette Sandholm Kastrup, Department of Medicinal Chemistry Danish University of Pharmaceutical Sciences, Universitetsparken 2, DK-2100, Copenhagen Ø, Denmark

Telephone: 45-3530-6486; Fax: 45-3530-6040; E-mail: jsk@dfuni.dk

Number of text pages: 38

Number of tables: 2

Number of figures: 7 (3 color figures)

Number of references: 43

Number of words in abstract: 256

Number of words in introduction: 880

Number of words in discussion: 1573 (including headings)

Abbreviations

ACPA, 2-amino-3-(3-carboxy-5-methylisoxazol-4-yl) propionic acid; AMPA, 2-amino-3-(3-hydroxy-5-methylisoxazol-4-yl) propionic acid; Br-HIBO, 2-amino-3-(4-bromo-3-hydroxy-isoxazol-5-yl) propionic acid; Br-Will, 5-bromo-willardiine; CPW399, 2-amino-3-(1,3,5,6,7-pentahydro-2,4-dioxo-cyclopenta[*e*]pyrimidin-1-yl) propanoic acid; F-Will, 5-fluoro-willardiine; Glu, glutamic acid; GluR2; AMPA-subtype ionotropic glutamate receptor 2; GluR2-S1S2J, soluble construct of the ligand-binding core of GluR2; iGluR, ionotropic glutamate receptor; I-Will, 5-iodo-willardiine; KA, kainic acid; MeTetAMPA, 2-amino-3-[3-hydroxy-5-(2-methyl-2*H*-tetrazol-5-yl)isoxazol-4-yl] propionic acid; [^{3}H]AMPA, (*RS*)-[5-methyl-^{3}H]-AMPA; rmsd, root mean square deviation; Will, willardiine

Molecular Pharmacology Fast Forward. Published on December 9, 2004 as DOI: 10.1124/mol.104.002931
This article has not been copyedited and formatted. The final version may differ from this version.

Abstract

Ionotropic glutamate receptors mediate most rapid excitatory synaptic transmission in the mammalian central nervous system and their involvement in neurological diseases has stimulated widespread interest in their structure and function. Despite a large number of agonists developed to date, few display selectivity among AMPA-receptor subtypes. The present study provides X-ray structures of the GluR2-selective, partial agonist (*S*)-2-amino-3-(1,3,5,6,7-pentahydro-2,4-dioxo-cyclopenta[(*e*]pyrimidin-1-yl) propanoic acid [(*S*)-CPW399] in complex with the ligand-binding core of GluR2 (GluR2-S1S2J) and with a (Y702F)GluR2-S1S2J mutant. In addition, the structure of the non-selective partial agonist kainate in complex with (Y702F)GluR2-S1S2J was determined. The results show that the selectivity of (*S*)-CPW399 towards full-length GluR2 relative to GluR3 is reflected in the binding data on the two soluble constructs, allowing the use of (Y702F)GluR2-S1S2J as a model system for studying GluR2/GluR3 selectivity. Structural comparisons suggest that selectivity arises from disruption of a water-mediated network between ligand and receptor. A D1-D2 domain closure occurs upon agonist binding. (*S*)-CPW399 and kainate induce greater domain closure in the Y702F mutant, indicating that these partial agonists here act in a manner more reminiscent of full agonists. Functionally, both kainate and (*S*)-CPW399 exhibited higher efficacy at (Y702F)GluR2(Q)$_i$ than at wild-type GluR2(Q)$_i$. Whereas an excellent correlation exists between domain closure and efficacy of a range of agonists at full-length GluR2, determined by electrophysiology in *Xenopus lævis oocytes*, a direct correlation between agonist induced domain closure of (Y702F)GluR2-S1S2J and efficacy at the GluR3 receptor is not observed. While clearly controlling selectivity, mutation of this residue alone is insufficient to explain agonist-induced conformational rearrangements occurring in this variant.

Molecular Pharmacology Fast Forward. Published on December 9, 2004 as DOI: 10.1124/mol.104.002931
This article has not been copyedited and formatted. The final version may differ from this version.

Introduction

Binding of (*S*)-glutamate to ionotropic glutamate receptors (iGluRs) is a key step in the predominant mechanism of rapid excitatory synaptic transmission among nerve cells within the mammalian central nervous system. iGluRs are important in the development and function of the central nervous system and are implicated in learning and memory formation. Furthermore, iGluRs also seem to be associated with certain neurological and psychiatric diseases, e.g. Alzheimer-type diseases, Parkinson's disease, epilepsy, stroke, ALS and schizophrenia. Therefore, the iGluRs are considered potential drug targets (Dingledine et al, 1999; Bräuner-Osborne et al, 2000). The iGluRs have been divided into three different classes: the (*S*)-2-amino-3-(3-hydroxy-5-methylisoxazol-4-yl) propionic acid (AMPA), kainic acid (KA) and *N*-methyl-D-aspartic acid (NMDA) receptors (Bräuner-Osborne et al, 2000). The AMPA receptor class consists of the subtypes GluR1-4. These can all exist in two different alternatively spliced isoforms named flip and flop (indicated by the subscripts i and o, respectively), which have different desensitization properties. In addition, the GluR2 subunit can exist in two different RNA-edited isoforms whereby a crucial amino-acid residue in the channel pore region can be either glutamine or arginine (the Q/R site) and this affects many channel properties, such as the rectification and ion-selectivity of GluR2-containing heteromeric channels (Dingledine et al, 1999).

The iGluRs form tetrameric ligand-gated ion channels (Rosenmund et al, 1998; Laube et al, 1998; Sun et al, 2002; Jin and Gouaux, 2003) (Fig. 1), and couple the energy of agonist binding to opening of a transmembrane ion pore (Dingledine et al, 1999). Two extracellular segments S1 and S2 have been shown to constitute the ligand-binding core (Fig. 1) and previous studies have shown that this ligand-binding core is necessary and

Molecular Pharmacology Fast Forward. Published on December 9, 2004 as DOI: 10.1124/mol.104.002931
This article has not been copyedited and formatted. The final version may differ from this version.

sufficient for achieving binding properties similar to that of the full-length membrane-bound receptor (Kuusinen et al, 1995; Chen and Gouaux, 1997). Soluble constructs of the ligand-binding core of the AMPA-receptor subunit GluR2 (GluR2-S1S2J) (Armstrong and Gouaux, 2000) and of the glycine-sensitive NMDA-subtype receptor NR1 (Furukawa and Gouaux, 2003) have been produced and structures of several agonists and antagonists in complex with these constructs have been reported in recent years (Hogner et al, 2002; Kasper et al, 2002; Hogner et al, 2003; Lunn et al, 2003; Jin et al, 2003). The ligands bind within a cleft formed by two domains (D1 and D2), where D1 is mainly composed of residues from segment S1 and D2 mainly of residues from S2.

The studies of Armstrong and Gouaux (2000) and Hogner et al (2002) have shown that AMPA receptor agonists with different efficacy induce distinct conformations of the ligand-binding core of GluR2 by inducing D1-D2 domain closure. A recent study on a series of complexes of 5-substituted willardiines has demonstrated that the size of a single substituent could control the degree of domain closure and thus lead to a range of ligand-dependent conformational states. Crystal structure determinations of a number of agonist complexes have shown that the constructs' conformational states are essentially unaffected by crystal packing and consequently the crystal structures of the constructs can serve as a model system for receptor-ligand binding (see e.g. Kasper et al, 2002; Lunn et al, 2003). Using single-channel recordings, these conformational states were shown to control the channel open probability of discrete subconductance states of the intact ion channel and thereby control receptor activation and also influen
ce receptor desensitization (Jin et al, 2003; Horning and Mayer, 2004).

Molecular Pharmacology Fast Forward. Published on December 9, 2004 as DOI: 10.1124/mol.104.002931
This article has not been copyedited and formatted. The final version may differ from this version.

Previously determined structures of GluR2-S1S2J complexes have revealed that a total of ca. 20 amino-acid residues from both D1 and D2 are in close proximity to the bound agonist (Lunn et al, 2003). Of these residues, all except Tyr702 are conserved among AMPA receptors. Banke et al (2001) identified this non-conserved Tyr residue in AMPA preferring subunits as being the main contributor to the selectivity of (*S*)-Br-HIBO for GluR1 over GluR3. In GluR1 this residue is conserved (Tyr698), whereas it is a phenylalanine (Phe706) in GluR3. We have previously reported the structure of a single-point mutant of the GluR2-S1S2J construct, (Y702F)GluR2-S1S2J, in complex with (*S*)-Br-HIBO and with (*S*)-ACPA (Hogner et al, 2002). A comparison of the structure of (*S*)-Br-HIBO complexed to GluR2-S1S2J with its (Y702F)GluR2-S1S2J complex greatly advanced early insights into the molecular mechanisms of AMPA receptor subtype selectivity.

Despite the large number of AMPA receptor agonists synthesised to date, very few have shown subtype selectivity. These agonists may be classified into two groups: AMPA-related analogs, e.g. (*S*)-Br-HIBO (Coquelle et al, 2000) and willardiine-like compounds, e.g. (*S*)-2-amino-3-(1,3,5,6,7-pentahydro-2,4-dioxo-cyclopenta[*e*]pyrimidin-1-yl) propanoic acid ((*S*)-CPW399) (Campiani et al, 2001), see Figure 2. These compounds show a certain degree of selectivity for GluR1/R2 over GluR3/R4, while ligands with significant selectivity for GluR3/R4 over GluR1/R2 remain elusive. The structures of the selective, partial agonist (*S*)-CPW399 in complex with GluR2-S1S2J and with the (Y702F)GluR2-S1S2J mutant are presented in addition to the structure of the non-selective, partial agonist KA in complex with (Y702F)GluR2-S1S2J. Binding affinities of (*S*)-CPW399 and KA for the ligand-binding core constructs have been compared with their affinities at full-length receptors. Furthermore, the efficacies of a range of

Molecular Pharmacology Fast Forward. Published on December 9, 2004 as DOI: 10.1124/mol.104.002931
This article has not been copyedited and formatted. The final version may differ from this version.

chemically distinct ligands have been determined (Fig. 2) at full-length GluR2, (Y702F)GluR2 and GluR3 receptors, ranging from the full agonist ACPA to the partial agonist KA, for comparison of their complexes with GluR2-S1S2J and (Y702F)GluR2-S1S2J. Such information may greatly facilitate the process of designing new AMPA receptor agonists and partial agonists with enhanced or novel selectivity profiles.

Material and Methods

Materials

(*S*)-CPW399, (*RS*)-ACPA and (*S*)-MeTetAMPA were synthesised as previously described (Campiani et al, 2001; Madsen and Wong, 1992; Bang-Andersen et al, 1997). (*RS*)-AMPA, (*RS*)-willardiine and halo-willardiine analogs were purchased from Tocris Cookson (Bristol, UK). (*RS*)-Br-HIBO was from Precision Biochemicals Inc. (Vancouver, Canada). Kainic acid and other chemicals were purchased from Sigma-Aldrich (Vallensbæk Strand, Denmark).

Protein Expression and Purification

Two constructs were used: The GluR2-S1S2J construct described by Armstrong and Gouaux (2000) was expressed, refolded and purified essentially as reported (Chen and Gouaux, 1997; Chen et al, 1998) while the synthesis of the GluR3-like construct, the single-point mutant (Y702F)GluR2-S1S2J, has been previously described (Hogner et al, 2002). Amino-acid nomenclature here refers to the mature protein sequence lacking the signal peptide.

Co-Crystallization of GluR2-S1S2J and (Y702F)GluR2-S1S2J with (*S*)-CPW399

Molecular Pharmacology Fast Forward. Published on December 9, 2004 as DOI: 10.1124/mol.104.002931
This article has not been copyedited and formatted. The final version may differ from this version.

The protein constructs were concentrated to 8 and 10 mg/mL for GluR2-S1S2J and (Y702F)GluR2-S1S2J, respectively, in the buffer also used for crystallization (10 mM HEPES pH 7.0, 20 mM NaCl, 1 mM EDTA) and saturated with the ligand (*S*)-CPW399 by adding the ligand in a 1:25 ratio to both constructs. Crystals were obtained at 6°C using the method of hanging drop vapor diffusion. A 1µL:1µL ratio of protein solution and reservoir buffer was used, over a 500 µL reservoir consisting of 0.2 M ammonium sulfate, 0.2 M cacodylate buffer pH 5.5 and 12% PEG 8000 for the GluR2-S1S2J:(*S*)-CPW399 crystals, while crystals of (Y702F)GluR2-S1S2J:(*S*)-CPW399 were obtained using 0.1 M ammonium sulfate, 0.1 M cacodylate buffer pH 6.5 and 16% PEG 8000 as reservoir. The crystals appeared within one week and grew to a maximum dimension of 0.1 mm. Crystals were soaked in cryo-protectant prior to flash-cooling in liquid nitrogen, using buffers as above but with the addition of 20% glycerol.

Co-Crystallization of (Y702F)GluR2-S1S2J with KA

(Y702F)GluR2-S1S2J was concentrated to 7.5 mg/mL in the crystallization buffer described above and saturated with KA by adding the ligand in a 1:38 ratio. Crystals were obtained at 6°C with the hanging drop vapor diffusion method using a reservoir solution consisting of 0.2 M lithium sulfate, 0.1 M cacodylate buffer pH 6.5 and 14% PEG 1000. Crystals were soaked in cryo-protectant prior to flash-cooling using reservoir buffer containing 20% glycerol.

X-ray Data Collection

The data from all complexes, GluR2-S1S2J in complex with (*S*)-CPW399 as well as the (Y702F)GluR2-S1S2J:(*S*)-CPW399 and (Y702F)GluR2-S1S2J:KA complexes, were

Molecular Pharmacology Fast Forward. Published on December 9, 2004 as DOI: 10.1124/mol.104.002931
This article has not been copyedited and formatted. The final version may differ from this version.

collected at a temperature of 100 K on a MAR CCD detector at beamline X11 (DESY, Hamburg, Germany) using a wavelength of 0.811 Å. The HKL package (Denzo, XdisplayF and Scalepack) (Otwinowski and Minor, 1997) was used for autoindexing, integration and scaling of the data (for statistics on data collections, see Table 1).

Structure Determination and Refinements

All structures were solved by molecular replacement, using the program AMoRe (Navaza, 1994) via the CCP4i interface (Collaborative Computational Project, Number 4, 1994). As a search model for the phasing of the GluR2-S1S2J:(*S*)-CPW399 data, the structure of GluR2-S1S2J in complex with Br-HIBO (Hogner et al, 2002) was employed, using only the protein atoms of the model. Phasing of the (Y702F)GluR2-S1S2J:(*S*)-CPW399 model was done using the GluR2-S1S2J:(*S*)-CPW399 as search model. In both cases, clear solutions to the rotation and translation functions occurred. ARP/wARP (Perrakis et al, 1999) was used for tracing of the entire structures, with the exception of three N-/C-terminal residues.

Ligand co-ordinates were calculated as follows and used for model building into electron densities and for generation of CNS topology and parameter files (Brünger et al, 1998). Firstly, the 1-methyl-1,2,3,5,6,7-hexahydro-cyclopenta[*e*]pyrimidin-4-one 2-olate was optimized using density functional theory (B3LYP) and the 6-311+G(d,p) basis set in Jaguar 4.2 (Macromodel V.8.0, Schrödinger Inc.: 1500 S. W. First Avenue, Suite 1180 Portland, OR 97201, USA), including PB-SCRF continuum aqueous solvation model, in order to obtain high quality co-ordinates for the geometry of the substituted ionized heterocycle in a polar environment. Both conformational enantiomers (due to slight puckering of the 5-membered ring) were generated. From this, two plausible low energy

Molecular Pharmacology Fast Forward. Published on December 9, 2004 as DOI: 10.1124/mol.104.002931
This article has not been copyedited and formatted. The final version may differ from this version.

bioactive conformations of (*S*)-CPW399 were built by replacing the 1-methyl with the appropriate zwitterionized (*S*)-alanine moiety. The side chain of each conformer was minimized with the MMFFs force field, including GB-SA treatment of aqueous solvation in Macromodel 8.0, while the positions of ring atoms and of those attached to the rings were kept frozen. The electron densities clearly defined the conformer with C6 ring puckering syn to the amino-acid side chain and it was modeled into the densities. This conformation of (*S*)-CPW399 is slightly lower in energy according to MMFFs. Most likely, it is the exact preferred dihedral about the side-chain heterocycle bond, which freezes the puckering mode of the 5-membered ring with a concomitant loss in entropy upon binding. The energy difference and inversion barrier is sufficiently low that the two are in rapid interconversion in solution.

Cycles of refinement and manual model building followed, using the program CNS for refinement and the program O (Jones et al, 1991) for visual inspection and model building. Positional and B-factor refinements as well as gradual inclusion of structural water molecules completed the model building.

The structure of GluR2-S1S2J in complex with KA (Armstrong and Gouaux, 2000) was used as a search model for determining the structure of the (Y702F)GluR2-S1S2J:KA complex. Only protein atoms were employed. One combined rotation and translation solution only was obtained from the molecular replacement run. ARP/wARP was used for tracing of the structure and resulted in an almost completely built model. Apart from one N-terminal residue and two other residues, all amino-acid residues were located. The resulting electron density of the ligand was very well defined and permitted an unequivocal positioning of KA in the structure. The co-ordinates of KA were extracted

Molecular Pharmacology Fast Forward. Published on December 9, 2004 as DOI: 10.1124/mol.104.002931
This article has not been copyedited and formatted. The final version may differ from this version.

from the pdb-file 1FW0. Refinements were carried out using the program REFMAC 5 (Murshudov et al, 1997), which contains parameters for KA, and manual model building was performed using the program O. Water molecules and sulfate ions were included gradually.

Using the numbering of the full-length (signal peptide removed) membrane-bound receptor, the resulting models of the (*S*)-CPW399 complexes include residues 392-506 from S1, a short linker consisting of the amino acids Gly and Thr, followed by residues 632-773 from S2. The final model of the (Y702F)GluR2-S1S2J:KA complex includes residues 393-506, the GT linker and residues 632-774. For a summary of refinement parameters, see Table 1.

Structure Analysis and Figure Preparation

To analyze domain closure, the program VMD (Wriggers and Schulten, 1997) was used, employing the HINGEFIND script (Wriggers and Schulten, 1997; Humphrey et al, 1997). The domain closure of each ligand–receptor complex was calculated relative to the apo structure of GluR2-S1S2J (pdb code 1FTO, MolA). The CCP4 routine CONTACTS was used to analyze protein-ligand interactions. Figures 1 and 5 were prepared using Molscript (Kraulis, 1991) and Raster3d (Merritt and Murphy, 1994).

Receptor Binding Assay

The affinities of (*S*)-CPW399 and KA for the GluR2-S1S2J and (Y702F)GluR2-S1S2J soluble constructs were determined by a radioligand binding assay. Purified construct (0.25 μg protein) was incubated with 2-3 nM (*RS*)-[5-methyl-^{3}H]-AMPA (43.5-55.5 Ci/mmol; Perkin Elmer, Boston, MA) in the presence of 1 nM–0.25 mM competitor for

1-2 hrs on ice in assay buffer (50 mM Tris-HCl, 100 mM KSCN, 2.5 mM $CaCl_2$, 10% glycerol pH 7.2 at 4°C). Samples were filtered onto Millipore (Billerica, MA) 0.22 μm GSWP nitrocellulose filters; the filters were washed twice with 2 mL cold assay buffer and radioactivity was determined by scintillation counting. Data were analyzed using Grafit v3.00 (Erithacus Software Ltd., Horley, UK) and fit as previously described (Nielsen et al, 1998) to determine Hill coefficient and K_i. The K_d values of [^{3}H]AMPA at GluR2-S1S2J (12.8 nM) and (Y702F)GluR2-S1S2J (17.1 nM) were previously determined (Hogner et al, 2002).

Electrophysiology

Mature female *Xenopus lævis* (African Reptile Park, Tokai, South Africa) were anesthetised using 0.1% ethyl 3-aminobenzoate methanesulfonate (tricaine) and ovaries were surgically removed. The ovarian tissue was dissected and treated with 2 mg/mL collagenase in nominally Ca^{2+}-free Barth's medium for 2 hrs at room temperature. On the second day, oocytes were injected with 25-50 nL of (~ 1 μg/μL) cRNA and incubated in Barth's medium (in mM: 88 NaCl, 1 KCl, 0.33 $Ca(NO_3)_2$, 0.41 $CaCl_2$, 0.82 $MgSO_4$, 2.4 $NaHCO_3$, 10 HEPES, pH 7.4) with 0.10 mg/mL gentamicin (Sigma) and 1% penicillin-streptomycin (Life Technologies, Paisley, UK) at 17ºC. Oocytes were typically used for recordings from 3–10 days post-injection and were voltage-clamped with the use of a two-electrode voltage clamp (GeneClamp 500B, Axon Instruments, Union City, CA) with both microelectrodes filled with 3 M KCl. Recordings were made while the oocytes were continuously superfused with Ca^{2+}-free frog Ringer's solution (in mM: 115 NaCl, 2 KCl, 1.8 $BaCl_2$, 5 HEPES, pH 7.0). Drugs were dissolved in Ca^{2+}-free frog Ringer's solution and added by bath application. Recordings were made at room temperature at

Molecular Pharmacology Fast Forward. Published on December 9, 2004 as DOI: 10.1124/mol.104.002931
This article has not been copyedited and formatted. The final version may differ from this version.

holding potentials in the range of -80 to -20 mV. All agonists were applied at saturating concentrations in the presence of 100 μM cyclothiazide in order to block receptor desensitization (cyclothiazide EC_{50}: GluR2(Q)$_i$ = 7.6 μM; GluR3$_i$ = 9.0 μM (Quirk and Nisenbaum, 2003; Varney et al., 1998). As a control for current rundown, oocytes were stimulated with (*S*)-glutamate (1 mM for GluR2(Q)$_i$ and GluR3$_i$; 2 mM for (Y702F)GluR2(Q)$_i$) plus 100 μM cyclothiazide immediately prior to each drug application, with a washout period of 5-10 min between applications. The drug maximum response was then expressed as a percentage of the test (*S*)-glutamate stimulation, assuming (*S*)-glutamate to be a full agonist and that rundown was not significant during the wash interval.

Molecular Biology

The rat AMPA receptor clones GluR2(Q)$_i$ and GluR3$_i$ within the vector pGEMHE (Liman et al, 1992) were used for preparation of high-expression cRNA transcripts. The GluR2(Q)$_i$ and GluR3$_i$ subtypes were selected since the *Q*-isoform of GluR2 allows for functional homomeric channels and the flip isoforms have greatest sensitivity to the desensitization-blocking drug cyclothiazide. For functional studies, the mutant (Y702F)GluR2(Q)$_i$pGEMHE was created by subcloning a 137 bp *BamH I- BspE I* DNA fragment from (Y702F)GluR2$_o$-S1S2JpET30a(+) (Hogner et al, 2002) into the wild-type GluR2(Q)$_i$pGEMHE. The mutation was verified by automated DNA sequencing of the cDNA (MWG Biotech AG, Ebersberg, Germany). cDNAs were grown in XL1 Blue bacteria (Stratagene, La Jolla, CA) and prepared using column purification (Qiagen, Chatsworth, CA). cRNA was synthesised from these cDNAs using the mMessage mMachine T7 mRNA-capping transcription kit (Ambion Inc., Austin, TX). Restriction

Molecular Pharmacology Fast Forward. Published on December 9, 2004 as DOI: 10.1124/mol.104.002931
This article has not been copyedited and formatted. The final version may differ from this version.

and other molecular biological enzymes were obtained from New England BioLabs (Beverly, MA).

Data Analysis of Pharmacology

One-way ANOVA (followed by the Bonferroni t-test) was utilized for comparison of efficacies using SigmaStat for Windows v3.0 (SPSS Inc., Chicago, IL). Values are given as means ± SEM and were considered statistically significantly different if $P < 0.05$. Concentration-response curves for agonists were analysed using Grafit v3.00 to determine the EC_{50} and Hill value (n_H), using the logistic equation:

$I = I_{max}/(1 + 10^{(\log[EC_{50}])}/10^{(\log [Agonist])})^{n_H}$, where I is the measured current and I_{max} is the maximal steady-state current.

Results

The present study was conducted to elucidate AMPA receptor agonist binding and selectivity at the molecular level. X-ray structures of the ligand-binding core of GluR2 in complex with two agonists have been determined: the structures of (*S*)-CPW399 in complex with GluR2-S1S2J and with the GluR3-like (Y702F)GluR2-S1S2J mutant, as well as the (Y702F)GluR2-S1S2J:KA complex have been characterized. The crystals of the GluR2-S1S2J:(*S*)-CPW399, (Y702F)GluR2-S1S2J:(*S*)-CPW399 and (Y702F)GluR2-S1S2J:KA diffracted to 1.8, 2.1 and 1.85 Å resolution, respectively (see Table 1). In addition, the binding pharmacology for (*S*)-CPW399 and KA at these constructs has been determined. Electrophysiology was employed to determine the relative efficacies of a series of chemically distinct AMPA-receptor agonists (Fig. 2) at full-length GluR2(Q)$_i$,

Molecular Pharmacology Fast Forward. Published on December 9, 2004 as DOI: 10.1124/mol.104.002931
This article has not been copyedited and formatted. The final version may differ from this version.

(Y702F)GluR2(*Q*)$_i$ and GluR3$_i$ expressed in *Xenopus lævis* oocytes, allowing for a direct study of the relation between ligand-binding core structure and efficacy.

Binding Pharmacology

The affinities of (*S*)-CPW399 at the GluR2-S1S2J construct (K_i = 393 ± 54 nM, n_H = 0.89 ± 0.03, n = 4) and at the (Y702F)GluR2-S1S2J construct (K_i = 3,330 ± 160 nM, n_H = 0.99 ± 0.03, n = 3) (Fig. 3A) are similar to those for GluR2(*R*)$_o$ and GluR3$_o$ (K_i = 218 ± 16 nM and K_i = 2,137 ± 218 nM, respectively) (Campiani et al, 2001). The affinity of KA at the (Y702F)GluR2-S1S2J construct (K_i = 624 ± 23 nM, n_H = 1.05 ± 0.09, n = 3) (Fig. 3A) is similar to that at GluR3$_o$ (K_i = 1,980 nM; (Nielsen et al, 1998)). However, the K_i values of (*S*)-CPW399 and KA at (Y702F)GluR2-S1S2J vs. GluR3$_o$, respectively, were statistically significantly different.

Functional Pharmacology

The relative efficacies of a series of AMPA receptor agonists (Fig. 2) were determined at GluR2(*Q*)$_i$ and GluR3$_i$ expressed in *X. lævis* oocytes, setting the endogenous ligand, (*S*)-glutamate, as a full agonist (Fig. 4). Desensitization of the responses was blocked by co-application of a saturating concentration of cyclothiazide (100 μM) in the presence of a saturating concentration (≥ 22-fold EC_{50}) of agonist. The EC_{50} values of the agonists used have been previously reported (Banke et al, 1997; Coquelle et al, 2000; Vogensen et al, 2000; Kizelsztein et al, 2000; Campiani et al, 2001). The efficacies of KA and (*S*)-CPW399 relative to (*S*)-glutamate were measured at GluR2(*Q*)$_i$: KA = 0.212 ± 0.032 (n = 19), (*S*)-CPW399 = 0.432 ± 0.036 (n = 21) and GluR3$_i$: KA = 0.242 ± 0.015 (n = 21), (*S*)-CPW399 = 0.147 ± 0.017 (n = 12). (*S*)-CPW399 gives a response at GluR2(*Q*)$_i$ in

Molecular Pharmacology Fast Forward. Published on December 9, 2004 as DOI: 10.1124/mol.104.002931
This article has not been copyedited and formatted. The final version may differ from this version.

between those observed for (*RS*)-Br-HIBO and KA. At $GluR3_i$, the efficacy of (*S*)-CPW399 is diminished compared to KA; (*S*)-CPW399 being the least efficacious agonist at $GluR3_i$ tested in this study. Hence, the rank ordering of efficacy of a series of agonists is not necessarily the same amongst the different AMPA receptors.

For direct comparison to the structures with complexes of (Y702F)GluR2-S1S2J, the efficacy of (*S*)-CPW399 and KA was also determined at the mutant (Y702F)GluR2$(Q)_i$. Concentration-response curves at (Y702F)GluR2$(Q)_i$ gave (mean ± SEM): (*S*)-glutamate: EC_{50} = 47 ± 3 μM, n_H = 0.87 ± 0.02, (n = 10); KA: EC_{50} = 129 ± 9 μM, n_H = 0.80 ± 0.01, (n = 10) and (*S*)-CPW399: EC_{50} = 43.7 ± 4.1 μM, n_H = 0.68 ± 0.02, (n = 8), (Fig. 3B). For measurement of the efficacies of KA and (*S*)-CPW399 compared to (*S*)-glutamate at this mutant the following saturating concentrations of agonists were utilized in the presence of 100 μM cyclothiazide: 2 mM (*S*)-glutamate, 5 mM KA and 4 mM (*S*)-CPW399. This gave the relative efficacy of KA as 0.468 ± 0.023 (n = 14) and (*S*)-CPW399 as 0.452 ± 0.043 (n = 19).

X-ray Structures of (*S*)-CPW399 Complexes with GluR2-S1S2J and (Y702F)GluR2-S1S2J

In the structure of the GluR1/GluR2 selective agonist (*S*)-CPW399 in complex with GluR2-S1S2J, one molecule is present in the asymmetric unit of the crystal. In the (Y702F)GluR2-S1S2J complex, two molecules are present, denoted MolA and MolB (rmsd of 0.22 Å on 259 Cα atoms). The mutation of Tyr702 to Phe leads to only minor changes in the local protein environment (rmsd of 0.52 Å on 259 Cα atoms). However, the D1-D2 domain closures differ by ca. 1°, increasing from 17.0° in GluR2-S1S2J to ca.

Molecular Pharmacology Fast Forward. Published on December 9, 2004 as DOI: 10.1124/mol.104.002931
This article has not been copyedited and formatted. The final version may differ from this version.

18.3° in the Y702F mutant structure (MolA: 18.2° and MolB: 18.3°). This increase in domain closure does not result in a flip of the Asp651-Ser652 peptide bond, which in both complexes adopts the conformation observed in the apo structure of GluR2-S1S2J (Armstrong and Gouaux, 2000).

(*S*)-CPW399 binds to a cleft between D1 and D2 (Fig. 1 and 5) in the vicinity of residues Glu402, Tyr405, Tyr450, Pro478-Thr480, Arg485 and Tyr732 from D1 and residues Leu650, Ser652-Lys656, Thr686, Tyr/Phe702, Leu704, Glu705 and Met708 from D2 (distance from (*S*)-CPW399 atoms to protein atoms < 5 Å). In both the GluR2-S1S2J and (Y702F)GluR2-S1S2J structures, the α-amino acid part of (*S*)-CPW399 binds to the ligand-binding core of GluR2 in the same manner as has been observed for several other agonist structures (Armstrong and Gouaux, 2000; Hogner et al; 2002, Kasper et al, 2002; Jin et al, 2003). The α-ammonium and α-carboxylate groups form hydrogen bonds to residues in both D1 and D2, specifically to Pro478, Thr480, Arg485, Ser654 and Glu705 (Table 2 and Figures 5A and 5B).

Both of the oxygen (O1 and O2) atoms and the (N3) nitrogen atom of the 1*H*-cyclopentauracil moiety of (*S*)-CPW399 are engaged in hydrogen-bond formation to the D2 residues Ser654, Thr655 and Glu705 (Table 2 and Figures 5A and 5B). The (O1) oxygen atom binds directly to Ser654 and Thr655 as observed for the γ-carboxylate group of (*S*)-glutamate and the oxyanion of the 3-isoxazolol group of (*S*)-MeTetAMPA, whereas (*S*)-AMPA binds indirectly through a water molecule (Armstrong and Gouaux, 2000; Hogner et al, 2002; Kasper et al, 2002). In the GluR2-S1S2J:(*S*)-CPW399 complex, the (O2) oxygen atom forms a water-mediated hydrogen bond to the phenol

oxygen atom of Tyr702 and to the (Oγ1) atom of Thr686. Due to the mutation of Tyr702 to a phenylalanine, this water molecule (water 2, Table 2) is absent from the (Y702F)GluR2-S1S2J complex structure and thus this ligand—water—protein link has been eliminated (see Figures 5A-C). In both MolA and MolB of the (Y702F)GluR2-S1S2J structure, the point mutation results in a movement of the cyclopentauracil moiety of (*S*)-CPW399 closer towards another water molecule (water 3, Table 2), which now mediates contacts between the (O2) and (N2) atoms of (*S*)-CPW399, the nitrogen atom of Leu650 and the oxygen atom of Leu703. The water 3 molecule is also present in the GluR2-S1S2J:(*S*)-CPW399 complex and, in addition to the aforementioned protein contacts, it also interacts with the OH group of Tyr702. The distance from the (O2) atom of (*S*)-CPW399 to water 3 oxygen is 3.9 Å compared to 3.2 Å (MolB) in the mutant and from the N2 atom of (*S*)-CPW399 to water 3 it is 3.8 Å compared to 3.2 Å (MolB). Although this might indicate a gain in hydrogen-bond strength, this gain is much less than the loss upon disappearance of the water 2 molecule, as an optimal hydrogen bond (2.9 Å) between the (O2) atom of (*S*)-CPW399 and water 2 is lost (Table 2).

Among the residues in close proximity to bound (*S*)-CPW399, the side-chain conformation of Glu402 differs between the GluR2-S1S2J and (Y702F)GluR2-S1S2J structures (identical in MolA and MolB); this might have a bearing on the strength of the Glu402–Thr686 interdomain lock (Fig. 5D). In addition, Met503, being in the vicinity of the mutated residue Tyr702 and also of Leu704, displays different side-chain conformations (not shown).

X-ray Structure of the (Y702F)GluR2-S1S2J:KA Complex

Molecular Pharmacology Fast Forward. Published on December 9, 2004 as DOI: 10.1124/mol.104.002931
This article has not been copyedited and formatted. The final version may differ from this version.

The structure of the (Y702F)GluR2-S1S2J:KA complex contains only one molecule in the asymmetric unit. The α-amino acid portion of the molecule is engaged in the same hydrogen-bonding network as (*S*)-CPW399 and other agonists. The binding cleft of the KA structure contains one more additional water molecule than the (*S*)-CPW399 complexes (water 4, Table 2). This water molecule is positioned to act as a mimic of the (O2) atom of (*S*)-CPW399 and is involved in hydrogen-bonding patterns similar to those of the (*S*)-CPW399 (O2) atom.

Overall, the structure of the (Y702F)GluR2-S1S2J:KA complex is very similar to the complex between KA and the native GluR2 ligand-binding core (Armstrong and Gouaux, 2000). The structures superimpose with an rmsd of 0.62 Å on 258 Cα-atoms. The main difference originates from the movement of water 2 (Table 2 and Fig. 5E). Due to the Y702F mutation, the environment of D2 surrounding water 2 is now more hydrophobic and as a consequence this water molecule moves ca. 1.2 Å towards D1 (not shown). This results in a shorter (and thus stronger) hydrogen bond between water 2 and Thr686 (Oγ1) in D2 (2.6 vs. 3.0 Å) and also in a decrease in the distance between Thr686 and Glu402 forming the interdomain lock (2.7 vs. 3.3 Å). This in turn allows for greater D1-D2 domain closure. The domain closure is 15.3° in the (Y702F)GluR2-S1S2J:KA complex, compared to 13.1° in the native KA complex. Additionally, the side chain of Ser654, which is hydrogen bonded to KA, is present in two conformations in the Y702F mutant (Fig. 5E).

Discussion

Mechanism of Binding Selectivity

Molecular Pharmacology Fast Forward. Published on December 9, 2004 as DOI: 10.1124/mol.104.002931
This article has not been copyedited and formatted. The final version may differ from this version.

Only few agonists display selectivity among the four AMPA sensitive iGluRs (GluR1-GluR4). One of these compounds is (*S*)-CPW399 and we have shown here that the 8.5-fold difference in binding affinity of (*S*)-CPW399 at full-length GluR2 relative to GluR3 is also reflected in its differential binding to the GluR2 ligand-binding core constructs GluR2-S1S2J and (Y702F)GluR2-S1S2J (Fig. 3A).

To understand how the mutation of the amino-acid residue 702 influences the selectivity of (*S*)-CPW399 towards GluR2, we have determined and compared the structures of (*S*)-CPW399 in complex with GluR2-S1S2J and (Y702F)GluR2-S1S2J. Unlike (*S*)-CPW399, KA is a non-selective, partial agonist at AMPA receptors and it induces the smallest domain closure (13°) known to date among ligands capable of AMPA ion-channel activation (Armstrong and Gouaux, 2000). The structure of KA in complex with GluR2-S1S2J has previously been determined (Armstrong and Gouaux, 2000) and here we present the structure of this compound in complex with (Y702F)GluR2-S1S2J.
The α-substituents of the agonists (carboxylate and ammonium groups) bind in a similar manner to the ligand-binding cleft residues in all structures (Table 2). In the (Y702F)GluR2-S1S2J:(*S*)-CPW399 complex, the single-point mutation results in the disappearance of a central water molecule (water 2), which mediates contacts between (*S*)-CPW399 and the hydroxyl groups of Tyr702 and Thr686 in GluR2-S1S2J (Fig. 5A-C). Hence, an important water-mediated interaction between (*S*)-CPW399 and the ligand-binding core residues is eliminated in the Y702F mutant. Such a significant change in ligand environment serves to explain the lower binding affinity. This is in accordance with what has been observed for the binding of (*S*)-Br-HIBO (Hogner et al, 2002).

Molecular Pharmacology Fast Forward. Published on December 9, 2004 as DOI: 10.1124/mol.104.002931
This article has not been copyedited and formatted. The final version may differ from this version.

Comparing the structures of KA in complex with GluR2-S1S2J and the Y702F mutant, a hydrogen bond is also lost between water 2 and Tyr702 in the mutant structure, which seems however, to be compensated by the shortening of the hydrogen bonds between water 2 and Thr686 (Oγ1) and between Thr686 and Glu402 forming an interdomain lock. Unlike (*S*)-CPW399, KA shows similar binding affinities at both GluR2-S1S2J [1,803 nM, (Armstrong and Gouaux, 2000)] and the Y702F mutant (624 nM). In accordance with this, KA does not form a direct hydrogen bond to water 2 in either of the structures. Thus, the distal anion of KA is equally liganded by both receptors, implying no differential desolvation penalty.

In summary, our results and structural comparisons support the hypothesis that the observed differences in binding affinities towards different AMPA-type iGluRs in general are due to a disruption of a water-mediated network between ligand and receptor. While (*S*)-CPW399 loses some interactions lacking water 2 in the Y702F mutant, KA still makes the same indirect H-bonding contacts to water 2 (Figures 5B, 5E and 5F), although this water molecule has moved in the mutant structure.

Domain Closure of the Ligand-Binding Core

(*S*)-CPW399 adopts the same conformation upon binding to the ligand-binding core of GluR2 and to the Y702F mutant but induces greater D1-D2 domain closure in the mutant (18.3° vs. 17.0° in GluR2-S1S2J). Upon mutation of Tyr702 to a phenylalanine, the disruption of the water-mediated hydrogen-bonding network between Tyr702 and the ligand in GluR2-S1S2J allows for a ca. 1 Å movement of the Cα atom of Phe702 into the binding cleft (Fig. 5C). A similar change in domain closure occurs in the structure of the

Molecular Pharmacology Fast Forward. Published on December 9, 2004 as DOI: 10.1124/mol.104.002931
This article has not been copyedited and formatted. The final version may differ from this version.

(Y702F)GluR2-S1S2J:KA complex, in which domain closure increases to 15.3°, versus 13.1° in the GluR2-S1S2J complex. In the latter, the central water molecule (water 2) is still present, but the shifted position of water 2 in the mutant structure liberates some space in the ligand-binding cleft, which allows for increased domain closure compared to the native complex. Thus, it seems that the partial agonists (*S*)-CPW399 and KA behave more like full agonists at the Y702F mutant, within the paradigm linking domain closure to efficacy. Functional evaluation of the efficacy of KA and (*S*)-CPW399 at the mutant (Y702F)GluR2(*Q*)$_i$ did indeed reveal increased efficacy compared to wild-type GluR2(*Q*)$_i$ (Fig. 3B). Similarly, it has previously been shown that mutation of Leu650 in GluR2, to the smaller Thr residue yields a receptor at which the partial agonist KA becomes more potent and efficacious. In this case, the measured domain closure of the corresponding (L650T)GluR2-S1S2J construct is also larger (Armstrong et al, 2003). By contrast, the AMPA congeners (*S*)-ACPA and (*S*)-Br-HIBO both induce an unchanged degree of domain closure in the GluR2-S1S2J and (Y702F)GluR2-S1S2J constructs (Hogner et al, 2002), although the measured relative efficacies of both are somewhat lower at GluR3$_i$ than GluR2(*Q*)$_i$ (Fig. 4).

The structure and domain closure of GluR2-S1S2J in complex with (*S*)-CPW399 is very similar to that of the (*S*)-I-Will complex [pdb code 1MQG:MolA; (Jin et al, 2003)] with the iodine atom of I-Will positioned approximately where (C8) of the cyclopentauracil ring system of (*S*)-CPW399 is located. The rmsd of 258 Cα atoms is 0.39 Å and only small changes in the side-chain conformations of Glu402 and Leu650 are observed. By contrast, the structure of the (Y702F)GluR2-S1S2J:(*S*)-CPW399 complex clearly resembles that of GluR2-S1S2J: (*S*)-F-Will (rmsd of 0.43 Å), apart from the binding site water network. Previous studies on a series of 5-substituted willardiine complexes

Molecular Pharmacology Fast Forward. Published on December 9, 2004 as DOI: 10.1124/mol.104.002931
This article has not been copyedited and formatted. The final version may differ from this version.

showed that consecutively increasing the size of a single substituent can correspondingly reduce the degree of domain closure and lead to a range of ligand-dependent conformational states of the ligand-binding core and a range of agonist efficacies (Jin et al, 2003). In agreement with this, (*S*)-CPW399 gives similar domain closure as (*S*)-I-Will and the same measured efficacy at GluR2(Q)$_i$. However, in the present study we see that it is not only the structure of distinct ligand compounds that induce various conformational states. We have shown that changes in the protein itself (e.g. the present study of the mutation of a residue in the binding cleft) can give rise to the same conformational state of the receptor for chemically distinct agonists.

Domain Closure is Related to Agonist Efficacy in GluR2-S1S2J

On the basis of kinetic experiments (Abele et al, 2000), it has been suggested that upon binding to the ligand-binding core of GluR2, agonists first interact with D1 residues in a 2-step process. Subsequently, D2 moves to close over the ligand. The free energy of binding is translated into conformational strain, which is then mechanically transferred to the ion channel and ultimately induces pore opening.

The (*S*)-CPW399 and KA complexes crystallize as a dimer (Fig. 1) as previously observed in other complexes (Armstrong and Gouaux, 2000; Hogner et al, 2002). As a measure of the D2-D2 domain separation in the dimer upon binding of an agonist, we have calculated the distance between C_α atoms of the two Ile633 residues located in the vicinity of the Gly–Thr linker residues. This linker replaces the M1 and M2 transmembrane regions (Fig. 1). A comparison of D1-D2 domain closure and D2-D2 linker separation induced by (*S*)-CPW399, in addition to a series of chemically distinct ligands included in the present study, reveals a linear correlation between these two

Molecular Pharmacology Fast Forward. Published on December 9, 2004 as DOI: 10.1124/mol.104.002931
This article has not been copyedited and formatted. The final version may differ from this version.

features (Fig. 6A). Furthermore, we have compared D2-D2 linker separation with the agonist efficacy, which strongly suggests that domain closure, followed by separation of the D2 domains of the dimer, is related to channel opening for (*S*)-CPW399 and all other compounds tested under the same conditions (Fig. 6A).

Comparison of (Y702F)GluR2-S1S2J Domain Closure and Agonist Efficacy at GluR3

GluR2 and GluR3 show 88% sequence identity within the S1 and S2 regions and most of the few non-conserved residues (in total 29) are located on the surface. The only non-conserved residue in the vicinity of the bound ligands is Tyr702. To test whether domain closure of the (Y702F)GluR2-S1S2J mutant reproduces the behavior of the GluR3 ligand-binding core, we have measured and compared the efficacies at the full-length $GluR3_i$ receptor for four chemically and pharmacologically different agonists with the D2-D2 separation in (Y702F)GluR2-S1S2J (see Fig. 6B).

Whereas the correlation between domain closure and separation of the Ile633 residues in the dimer is excellent, no direct correlation between the D2-D2 separation of (Y702F)GluR2-S1S2J and efficacy at $GluR3_i$ appears (Fig. 6). In fact, KA has increased domain closure at (Y702F)GluR2-S1S2J versus GluR2-S1S2J, however, the measured efficacy at $GluR2(Q)_i$ is not different from $GluR3_i$. More interestingly, (*S*)-CPW399 has larger domain closure at (Y702F)GluR2-S1S2J versus GluR2-S1S2J, resembling the GluR2-S1S2J: (*S*)-F-Will complex, yet has an efficacy lower even than that of KA at $GluR3_i$. However, the efficacy of (*S*)-CPW399 (and KA) at the (Y702F)$GluR2(Q)_i$ mutant is as expected from the observed domain closure and D2-D2 separation, bringing the points back to the regression line (Fig. 6B). Therefore, mutation of Tyr702 to Phe

cannot solely account for conformational rearrangements induced within the ligand-binding core of GluR3 upon binding of an agonist. In light of this, we note some further sequence differences between the GluR3 binding-site mimic (Y702F)GluR2 and GluR3 that may be of functional importance (Fig. 7). Tyr702 is in proximity to Tyr700, which is also replaced by a Phe in GluR3. The Y700F mutation is known to affect the desensitization rate constant of GluR1 (Banke et al, 2001). Tyr700 is in contact with the loop on which the Gly-Thr linker is situated and which also includes residues Ala646-Tyr647 whose order is reversed in GluR3. These changes outside of the ligand-binding site create possibilities for differences in topography between GluR2 and GluR3. In conclusion, the coupling between domain closure and channel gating at non-GluR2 AMPA receptors may be somewhat different from that of GluR2 and a thorough understanding must await the determination of the structure and pharmacology of soluble constructs of the other subunits.

Molecular Pharmacology Fast Forward. Published on December 9, 2004 as DOI: 10.1124/mol.104.002931
This article has not been copyedited and formatted. The final version may differ from this version.

Acknowledgements

Eric Gouaux is kindly acknowledged for providing the GluR2-S1S2J construct and purification protocol and Lise B. Sørensen for technical assistance.

References

Abele R, Keinänen K and Madden DR (2000) Agonist-induced isomerization in a glutamate receptor ligand-binding domain. A kinetic and mutagenetic analysis. *J. Biol. Chem*. 275: 21355-21363.

Armstrong N and Gouaux E (2000) Mechanisms for activation and antagonism of an AMPA-sensitive glutamate receptor: Crystal structures of the GluR2 ligand binding core. *Neuron* 28: 165-181.

Armstrong N, Mayer M and Gouaux E (2003) Tuning activation of the AMPA-sensitive GluR2 ion channel by genetic adjustment of agonist-induced conformational changes. *Proc. Natl. Acad. Sci. U.S.A* 100: 5736-5741.

Bang-Andersen B, Lenz SM, Skjærbæk N, Søby KK, Hansen HO, Ebert B, Bøgesø KP and Krogsgaard-Larsen P (1997) Heteroaryl analogues of AMPA. Synthesis and quantitative structure-activity relationships. *J. Med. Chem.* 40: 2831-2842.

Banke TG, Schousboe A and Pickering DS (1997) Comparison of the agonist binding site of homomeric, heteromeric and chimeric $GluR1_o$ and $GluR3_o$ AMPA receptors. *J. Neurosci. Res.* 49: 176-185.

Banke TG, Greenwood JR, Christensen JK, Liljefors T, Traynelis SF, Schousboe A and Pickering DS (2001) Identification of amino acid residues in GluR1 responsible for ligand binding and desensitization. *J. Neurosci*. 21: 3052-3062.

Bräuner-Osborne H, Egebjerg J, Nielsen EØ, Madsen U and Krogsgaard-Larsen P (2000) Ligands for glutamate receptors: Design and therapeutic prospects. *J. Med. Chem*. 43: 2609-2645.

Brünger AT, Adams PD, Clore GM, DeLano WL, Gros P, Grosse-Kunstleve RW, Jiang JS, Kuszewski J, Nilges M, Pannu NS, Read RJ, Rice LM, Simonson T and Warren GL (1998) Crystallography & NMR system: A new software suite for macromolecular structure determination. *Acta Crystallogr*. D54: 905-921.

Campiani G, Morelli E, Nacci V, Fattorusso C, Ramunno A, Novellino E, Greenwood J, Liljefors T, Griffiths R, Sinclair C, Reavy H, Kristensen AS, Pickering DS, Schousboe A, Cagnotto A, Fumagalli E and Mennini T (2001) Characterization of the 1H-cyclopentapyrimidine-2,4(1H,3H)-dione derivative (S)-CPW399 as a novel, potent, and subtype-selective AMPA receptor full agonist with partial desensitization properties. *J. Med. Chem*. 44: 4501-4504.

Chen GQ and Gouaux E (1997) Overexpression of a glutamate receptor (GluR2) ligand binding domain in Escherichia coli: Application of a novel protein folding screen. *Proc. Natl. Acad. Sci. U.S.A.* 94: 13431-13436.

Chen GQ, Sun Y, Jin R and Gouaux E (1998) Probing the ligand binding domain of the GluR2 receptor by proteolysis and deletion mutagenesis defines domain boundaries and yields a crystallizable construct. *Protein Sci*. 7: 2623-2630.

Collaborative Computational Project, Number 4 (1994) The CCP4 suite: Programs for protein crystallography. *Acta Crystallogr.* D50: 760-763.

Coquelle T, Christensen JK, Banke TG, Madsen U, Schousboe A and Pickering DS (2000) Agonist discrimination between AMPA receptor subtypes. *Neuroreport*. 11: 2643-2648.

Dingledine R, Borges K, Bowie D and Traynelis SF (1999) The glutamate receptor ion channels. *Pharmacol. Rev*. 51: 7-61.

Furukawa H and Gouaux E (2003) Mechanisms of activation, inhibition and specificity: Crystal structures of the NMDA receptor NR1 ligand-binding core. *EMBO J*. 22: 2873-2885.

Hogner A, Kastrup JS, Jin R, Liljefors T, Mayer ML, Egebjerg J, Larsen IK and Gouaux E (2002) Structural basis for AMPA receptor activation and ligand selectivity: Crystal structures of five agonist complexes with the GluR2 ligand-binding core. *J. Mol. Biol*. 322: 93-109.

Hogner A, Greenwood JR, Liljefors T, Lunn M, Egebjerg J, Larsen IK, Gouaux E and Kastrup JS (2003) Competitive antagonism of AMPA receptors by ligands of different classes: Crystal structure of ATPO bound to the GluR2 ligand-binding core, in comparison with DNQX. *J. Med. Chem.* 46: 214-221.

Humphrey W, Dalke A and Schulten K (1997) VMD - Visual Molecular Dynamics. *J. Mol. Graphics* 14: 33-38.

Jin R and Gouaux E (2003) Probing the function, conformational plasticity, and dimer-dimer contacts of the GluR2 ligand-binding core: Studies of 5-substituted willardiines and GluR2 S1S2 in the crystal. *Biochemistry* 42: 5201-5213.

Jin R, Banke TG, Mayer ML, Traynelis SF and Gouaux E (2003) Structural basis for partial agonist action at ionotropic glutamate receptors. *Nat. Neurosci.* 6: 803-810.

Jones TA, Zou JY, Cowan SW and Kjeldgaard M (1991) Improved methods for binding protein models in electron density maps and the location of errors in these models. *Acta Crystallogr*. A47: 110-119.

Kasper C, Lunn M-L, Liljefors T, Gouaux E, Egebjerg J and Kastrup JS (2002) GluR2 ligand-binding core complexes: Importance of the isoxazolol moiety and 5-substituent for the binding mode of AMPA-type agonists. *FEBS Lett.* 531: 173-178.

Kizelsztein P, Eisenstein M, Strutz N, Hollmann M and Teichberg VI (2000) Mutant cycle analysis of the active and desensitized states of an AMPA receptor induced by willardiines. *Biochemistry* 39: 12819-12827.

Kleywegt GJ and Jones TA (1996) Phi/psi-chology: Ramachandran revisited. *Structure* 4: 1395-1400.

Kraulis PJ (1991) MOLSCRIPT: A program to produce both detailed and schematic plots of protein structures. *J. Appl. Crystallogr*. 24: 946-950.

Kuusinen A, Arvola M and Keinänen K (1995) Molecular dissection of the agonist binding site of an AMPA receptor. *EMBO J*. 14: 6327-6332.

Laube B, Kuhse J and Betz HJ (1998) Evidence for a tetrameric structure of recombinant NMDA receptors. *Neurosci.* 18: 2954-2961.

Liman ER, Tytgat J and Hess P (1992) Subunit stoichiometry of a mammalian K+ channel determined by construction of multimeric cDNAs. *Neuron* 9: 861-871.

Lunn M-L, Nielsen MM, Hogner A, Gouaux E, Egebjerg J and Kastrup JS (2003) Three-dimensional structure of the ligand-binding core of GluR2 in complex with the agonist (S)-ATPA: Implications for receptor subunit selectivity. *J. Med. Chem.* 46: 872-875.

Madsen U and Wong EH (1992) Heterocyclic excitatory amino acids. Synthesis and biological activity of novel analogues of AMPA. *J. Med. Chem.* 35: 107-111.

Merritt EA and Murphy MEP (1994) Raster3D Version 2.0--A Program for Photorealistic Molecular Graphics'. *Acta Crystallogr.* D50: 869-873.

Murshudov GN, Vagin AA and Dodson EJ (1997) Refinement of macromolecular structures by the maximum-likelihood method. *Acta Crystallogr*. D53**:** 240-255.

Navaza J (1994) AMoRe: An atomated package for molecular replacement. *Acta Crystallogr*. A50: 157-163.

Nielsen B, Banke TG, Schousboe A and Pickering DS (1998) Pharmacological properties of homomeric and heteromeric GluR1o and GluR3o receptors. *Eur. J. Pharmacol.* 360: 227-238.

Otwinowski Z and Minor W (1997) Processing of X-ray diffraction data collected in oscillation mode. *Methods Enzymol*. 276: 307-326.

Perrakis A, Morris R and Lamzin VS (1999) Automated protein model building combined with iterative structure refinement. *Nat. Struct. Biol*. 6: 458-463.

Quirk JC and Nisenbaum ES (2003) Multiple molecular determinants for allosteric modulation of alternatively spliced AMPA receptors. *J. Neurosci*. 23: 10953-10962.

Rosenmund C, Stern-Bach Y and Stevens CF (1998) The tetrameric structure of a glutamate receptor channel. *Science* 280: 1596-1599.

Sun Y, Olson R, Horning M, Armstrong N, Mayer M and Gouaux E (2002) Mechanism of glutamate receptor desensitization. *Nature* 417: 245-253.

Varney MA, Rao SP, Jachec C, Deal C, Hess SD, Daggett LP, Lin F, Johnson EC and Velicelebi G (1998) Pharmacological characterization of the human ionotropic glutamate

receptor subtype GluR3 stably expressed in mammalian cells. *J. Pharmacol. Exp. Ther*. 285: 358-370.

Vogensen SB, Jensen HS, Stensbøl TB, Frydenvang K, Bang-Andersen B, Johansen TN, Egebjerg J and Krogsgaard-Larsen P (2000) Resolution, configurational assignment, and enantiopharmacology of 2-amino-3-[3-hydroxy-5-(2-methyl-2H- tetrazol-5-yl)isoxazol-4-yl]propionic acid, a potent GluR3- and GluR4-preferring AMPA receptor agonist. *Chirality* 12: 705-713.

Wriggers W and Schulten K (1997) Protein domain movements: Detection of rigid domains and visualization of hinges in comparisons of atomic coordinates. *Proteins* 29: 1-14.

Molecular Pharmacology Fast Forward. Published on December 9, 2004 as DOI: 10.1124/mol.104.002931
This article has not been copyedited and formatted. The final version may differ from this version.

Footnotes

Database accession numbers

The structures have been deposited within the Protein Databank with accession numbers 1SYH, 1SYI and 1XHY.

Financial support

This work was supported by The Carlsberg Foundation, The Lundbeck Foundation, DANSYNC (Danish Centre for Synchrotron Based Research), Apotekerfonden of 1991, The Danish Medical Research Council, The Novo Nordisk Foundation, the computing resources of The Australian Centre for Advanced Computing and Communications as well as The Danish Center for Scientific Computing and the European Community – Access to Research Infrastructure Action of the Improving Human Potential Programme to the EMBL Hamburg Outstation, contract number HPRI-CT-1999-00017.

Figure legends

FIG. 1. Schematic representation of the tetrameric full-length GluR2 receptor. The structures of the two dimers of the ligand-binding core, (Y702F)GluR2-S1S2J, are shown in the colors red/orange and cyan/blue. Four (*S*)-CPW399 molecules are shown in cpk representation. Above the ligand-binding cores are schematic representations of the N-terminal domains. The transmembrane region forming the ion channel (represented as rods and color-coded as the corresponding ligand-binding core) is depicted below. The lipid bilayer is light grey.

FIG. 2. Chemical structures of iGluR agonists included in the present study. The atom numberings of (*S*)-CPW399 and KA used in Table 2 are shown in italics. See abbreviations for compound names.

FIG. 3. Pharmacological profiles of KA and (*S*)-CPW399. (A) Affinities of (*S*)-CPW399 and KA at the soluble AMPA receptor constructs representing the GluR2 (GluR2-S1S2J) and GluR3 ((Y702F)GluR2-S1S2J) binding sites. One representative [^{3}H]AMPA radioligand binding experiment is shown for each (means ± S.D. of triplicates). Each experiment was replicated a total of 3-4 times. ●, GluR2-S1S2J [(*S*)-CPW399: K_i = 487 nM for experiment shown]; ▲, (Y702F)GluR2-S1S2J [(*S*)-CPW399: K_i = 3,590 nM]; ■, (Y702F)GluR2-S1S2J (KA: K_i = 662 nM). (B) Potency of (*S*)-glutamate (●), KA (o) and (*S*)-CPW399 (□) at (Y702F)GluR2(Q)$_i$ expressed in *X. lævis* oocytes. Shown are single experiments (replicated 8-10 times) with responses normalized to the maximal steady-state current of each drug. EC_{50} (μM) for the shown curves: (*S*)-glutamate = 56; KA = 116; (*S*)-CPW399 = 32. *Inset*: Current traces for the shown KA concentration-response curve. The KA concentration (μM) is indicated above each response.

FIG. 4. Efficacy determinations relative to the full agonist (*S*)-glutamate. Shown are means ± SEM (n value indicated within bar) at: (A) GluR2(Q)$_i$ and (B) GluR3$_i$ using a saturating concentration of agonist in the presence of 100 μM cyclothiazide. Maximum agonist responses were determined and normalized to that of a preceding test stimulation of 1 mM (*S*)-glutamate + 100 μM cyclothiazide. Values in parentheses above each bar indicate which agonists are statistically significantly different (one-way ANOVA with Bonferroni t-test, $P < 0.05$).

FIG. 5. Binding modes of the ligands (*S*)-CPW399 and KA to GluR2-S1S2J and (Y702F)GluR2-S1S2J, including potential hydrogen bonds within 3.4 Å. (A) Close-up view of the GluR2-S1S2J:(*S*)-CPW399 complex. (B) Close-up view of the (Y702F)GluR2-S1S2J:(*S*)-CPW399 complex. (C) Superposition of the structures of (*S*)-CPW399 in complex with GluR2-S1S2J and (Y702F)GluR2-S1S2J. The water-mediated hydrogen-bonding network from ligand to Tyr702 in the GluR2-S1S2J complex is indicated. This network is absent in the Y702F mutant structure. (D) Overview of the structure of (Y702F)GluR2-S1S2J:(*S*)-CPW399, showing the orientation of the complexes. All structures are shown in similar orientations and are superimposed on D1 residues (Cα atoms). The hydrogen bond between Glu402 and Thr686 is shown, forming the interdomain lock. (E) Close-up view of the (Y702F)GluR2-S1S2J:KA complex. (F) Superposition of the structures of (*S*)-CPW399 and KA in complex with (Y702F)GluR2-S1S2J, respectively. The hydrogen-bonding network from KA to water 4 (W4) is shown. In (Y702F)GluR2-S1S2J, domain D1 is dark purple and D2 is dark green, whereas D1 is light purple and D2 is light green in GluR2-S1S2J. The side chain of Ser654 is located in two different conformations in the structures of GluR2-S1S2J:(*S*)-CPW399 and (Y702F)GluR2-S1S2J:KA. Oxygen atoms are colored red, nitrogen atoms are blue and

carbon atoms of ligands have been colored light and dark purple for the GluR2-S1S2J and (Y702F)GluR2-S1S2J complexes, respectively. In A, B and E, the water molecules are shown as red spheres, whereas in C they are colored light and dark purple for the GluR2-S1S2J and (Y702F)GluR2-S1S2J complexes and in E light and dark purple for (*S*)-CPW399 and KA complexes.

FIG. 6. Plot of (A) domain closure and (B) agonist efficacy at GluR2(*Q*)$_i$ versus the separation of an equivalent D2 residue (Ile633) in the ligand-binding core dimer of GluR2-S1S2J (o), (Y702F)GluR2(*Q*)$_i$ versus the separation in (Y702F)GluR2-S1S2J (▲) and GluR3$_i$ versus the separation in (Y702F)GluR2-S1S2J (●), upon binding of 11 agonists. In A, the bars show estimated standard deviations of domain closure where more than one protein molecule was present in the asymmetric unit of the crystal. The solid line shows a high positive correlation between domain closure and D2-D2 separation for both constructs. In B, the bars show standard errors of efficacy means. The solid line shows a positive correlation between GluR2(*Q*)$_i$ efficacy and GluR2-S1S2J D2-D2 separation. Compound numbering: 1: KA (pdb code 1FW0 and 1XHY); 2: CPW399 (1SYH and 1SYI); 3: Br-Will (1MQH); 4: Br-HIBO (1M5C and 1M5D); 5: F-Will (1MQI); 6: I-Will (1MY4); 7: Will (1MQJ); 8: Glu (1FTJ); 9: AMPA (1FTM); 10: ACPA (1M5E and 1M5F); and 11: MeTetAMPA (1M5B).

FIG. 7. Zoom on selected aromatic residues in domain 2, which are non-conserved between GluR2 (purple) and GluR3 (red) and which may be of functional importance.

TABLE 1

Crystallographic data and statistics of structure refinement

Data set	**GluR2:(*S*)-CPW399**	**(Y702F)GluR2:(*S*)-CPW399**	**(Y702F)GluR2:KA**
Source	X11, EMBL, Hamburg	X11, EMBL, Hamburg	X11, EMBL, Hamburg
Detector	MAR CCD	MAR CCD	MAR CCD
Space group	$P2_12_12$	$P4_1$	$P2_12_12$
Unit cell (Å)	a = 58.91, b = 96.35, c = 48.53	a=47.72, b=47.72, c=237.40	a=95.73, b=60.30, c=48.49
Solvent content (%)	48	47	42
No. per a. u.[a]	1	2	1
Oscillation (°)	0.5	0.5	0.5
Crystal mosaicity (°)	0.36	0.60	0.77
Wavelength (Å)	0.8111	0.8111	0.8111
Resolution (Å)[b]	24.4-1.8 (1.86-1.80)	20.0-2.1 (2.18-2.10)	20.4-1.85 (1.88-1.85)
Unique Obs.	26,350	28,467	24,433
Average redundancy	4.2	3.2	3.5
Completeness (%)[b]	99.3 (100)	92.3 (90.2)	98.9 (96.0)
Rmerge (%)[b]	9.0 (39.2)	8.6 (34.7)	7.3 (43.2)
$I/\sigma(I)$[b]	14.8 (3.5)	10.3 (3.3)	16.1 (3.0)
Refinement			
Atoms in structure	2,511	4,458	2,456
No. of waters and sulfate ions	421/0	372/0	361/5
R-factor (%)[c]	18.0	20.2	15.4
R-free (%)[d]	20.1	25.0	20.7
Rmsd bond lengths (Å)/angles (º)	0.008/1.4	0.006/1.2	0.02/1.8
Residues in allowed regions of Ramachandran plot (%)[e]	99.6	98.7	100
Average B-factors of main-chain atoms ($Å^2$)	8.5	22.1	16.0
Average B-factors of side-chain atoms ($Å^2$)	11.8	25.1	20.0
Average B-factors of waters and sulfate ions ($Å^2$)	26.4/-	31.8/-	31.9/52.3

Molecular Pharmacology Fast Forward. Published on December 9, 2004 as DOI: 10.1124/mol.104.002931
This article has not been copyedited and formatted. The final version may differ from this version.

[a] Number of protein molecules per asymmetric unit (a.u.).
[b] Values in parentheses correspond to the highest resolution bin.
[c] Crystallographic R-factor = $\sum_{(hkl)} \left\| F_o \right| - \left| F_c \right\| \Big/ \sum_{(hkl)} \left| F_o \right|$.

[d] R-free = $\sum_{(hkl)\in T} \left\| F_o \right| - \left| F_c \right\| \Big/ \sum_{(hkl)\in T} \left| F_o \right|$ where T is a test set containing a random 5.0, 2.5 and 5.0% of the observations omitted from the refinement process for the GluR2-S1S2J:(*S*)-CPW399, (Y702F)GluR2-S1S2J:(*S*)-CPW399 and (Y702F)GluR2-S1S2J:KA complexes, respectively.

[e] The Ramachandran plots were calculated according to Kleywegt and Jones (1996).

TABLE 2

Interactions of the ligand-binding core of GluR2-S1S2J/(Y702F)GluR2-S1S2J with (S)-CPW399 and KA. Potential hydrogen bonds/ionic interactions (in Å) to ligand within 3.4 Å are tabulated.

	GluR2: (*S*)-CPW399	**(Y702F)GluR2: (*S*)-CPW399**		**(Y702F)GluR2: KA**
		MolA[a]	**MolB**[a]	
O1[b]				
Ser654 N	3.4	3.3	3.1	3.0
Thr655 N	3.1	3.1	3.0	2.9
Thr655 Oγ1	3.2	3.0		3.3
Water 1	2.8	3.0	3.1	2.8
N2				
Thr655 Oγ1	2.8	2.7	2.7	2.5 (to O2 [c])
Water 3			3.2	3.1 (to O2 [c])
Water 4				2.7 (to O2 [c])
O2				
Glu705 N	2.9	2.9	3.0	
Water 2	2.9			
Water 3		3.4	3.2	
N3				
Pro478 O	2.8	2.7	2.8	3.0
Thr480 Oγ1	2.8	2.9	2.8	3.2
Glu705 Oε1	2.8	2.9	2.7	2.8
Glu705 Oε2	3.0	3.2	3.1	3.4
O3				
Arg485 Nη1		3.4	3.3	3.4
Arg485 Nη2	2.8	2.8	2.6	2.9
Ser654 N	2.9	2.9	3.1	2.9
Ser654 Oγ	2.9			2.9
O4				
Thr480 N	2.8	2.8	2.7	3.0
Thr480 Oγ1				3.3
Arg485 Nη1	2.8	2.7	2.7	2.9

[a](*S*)-CPW399 MolA and MolB refer to the two molecules in the asymmetric unit of the crystal.

[b]For atom numbering of (*S*)-CPW399 and KA, see Fig. 2.

[c]The position of the O2 atom of KA approximately corresponds to the position of the N2 atom of (*S*)-CPW399 (1.2 Å apart).

Figure 1

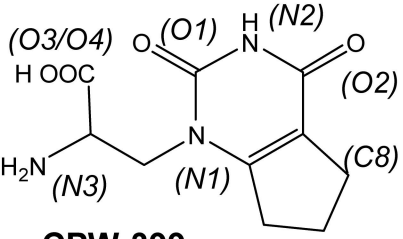

CPW-399

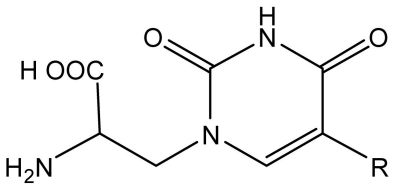

	R
Will	H
F-Will	F
Br-Will	Br
I-Will	I

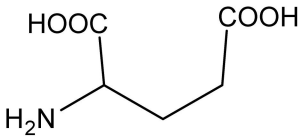

Glutamate

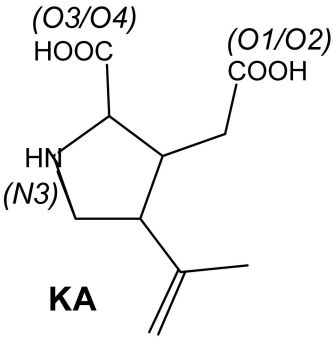

KA

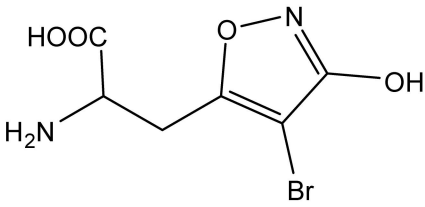

Br-HIBO

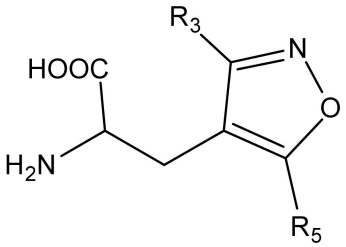

	R_3	**R_5**
ACPA	COOH	CH_3
AMPA	OH	CH_3
MeTetAMPA	OH	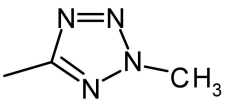

Figure 2

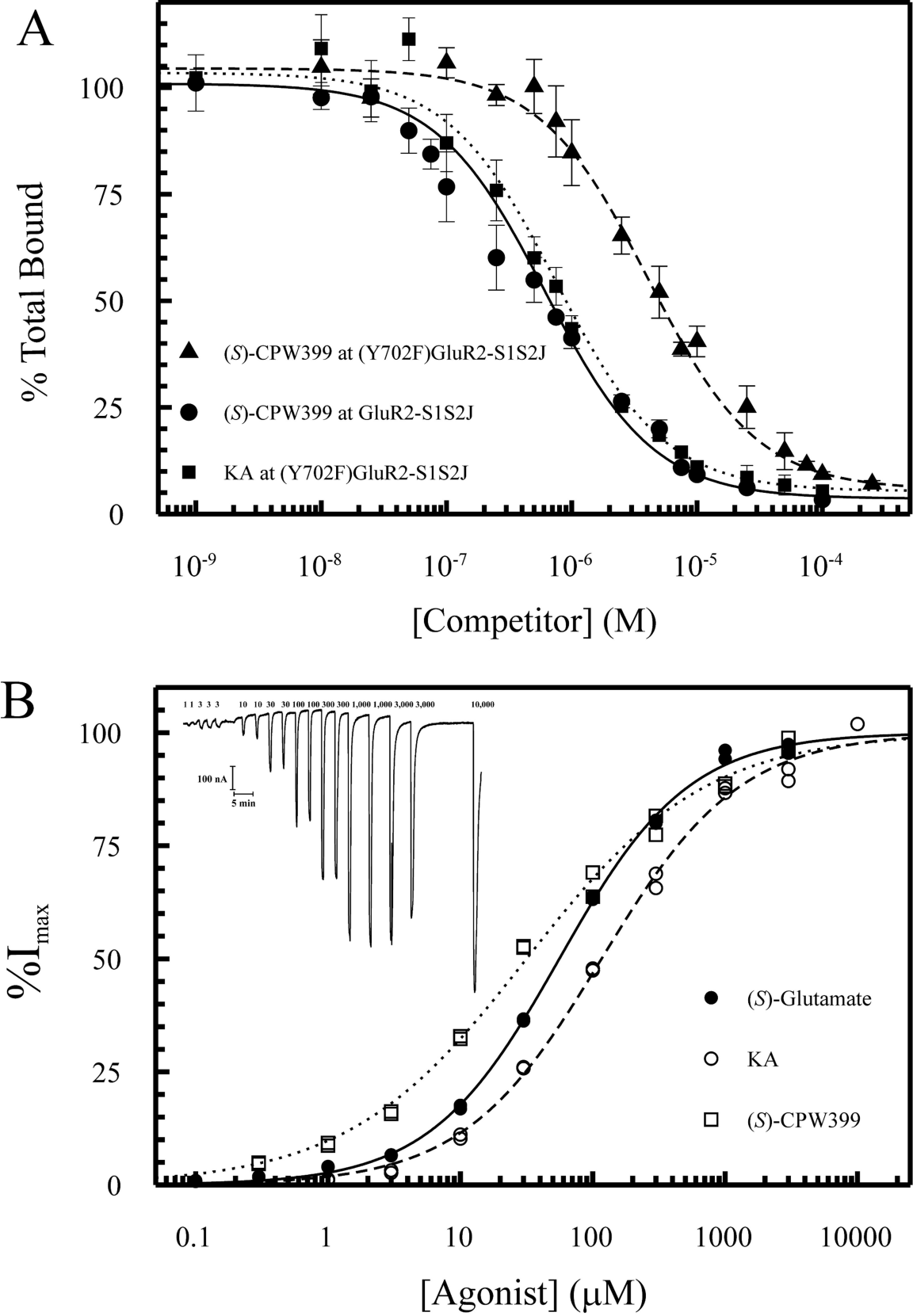
A
100
75
50
25
0
% Total Bound
(S)-CPW399 at (Y702F)GluR2-S1S2J
(S)-CPW399 at GluR2-S1S2J
KA at (Y702F)GluR2-S1S2J
10-9
10-8
10-7
10-6
10-5
10-4
[Competitor] (M)
B
100
75
50
25
0
%Imax
1 1 3 3 3 10 10 30 30 100 100 300 300 1,000 1,000 3,000 3,000 10,000
100 nA
5 min
(S)-Glutamate
KA
(S)-CPW399
0.1
1
10
100
1000
10000
[Agonist] (μM)

Figure 3

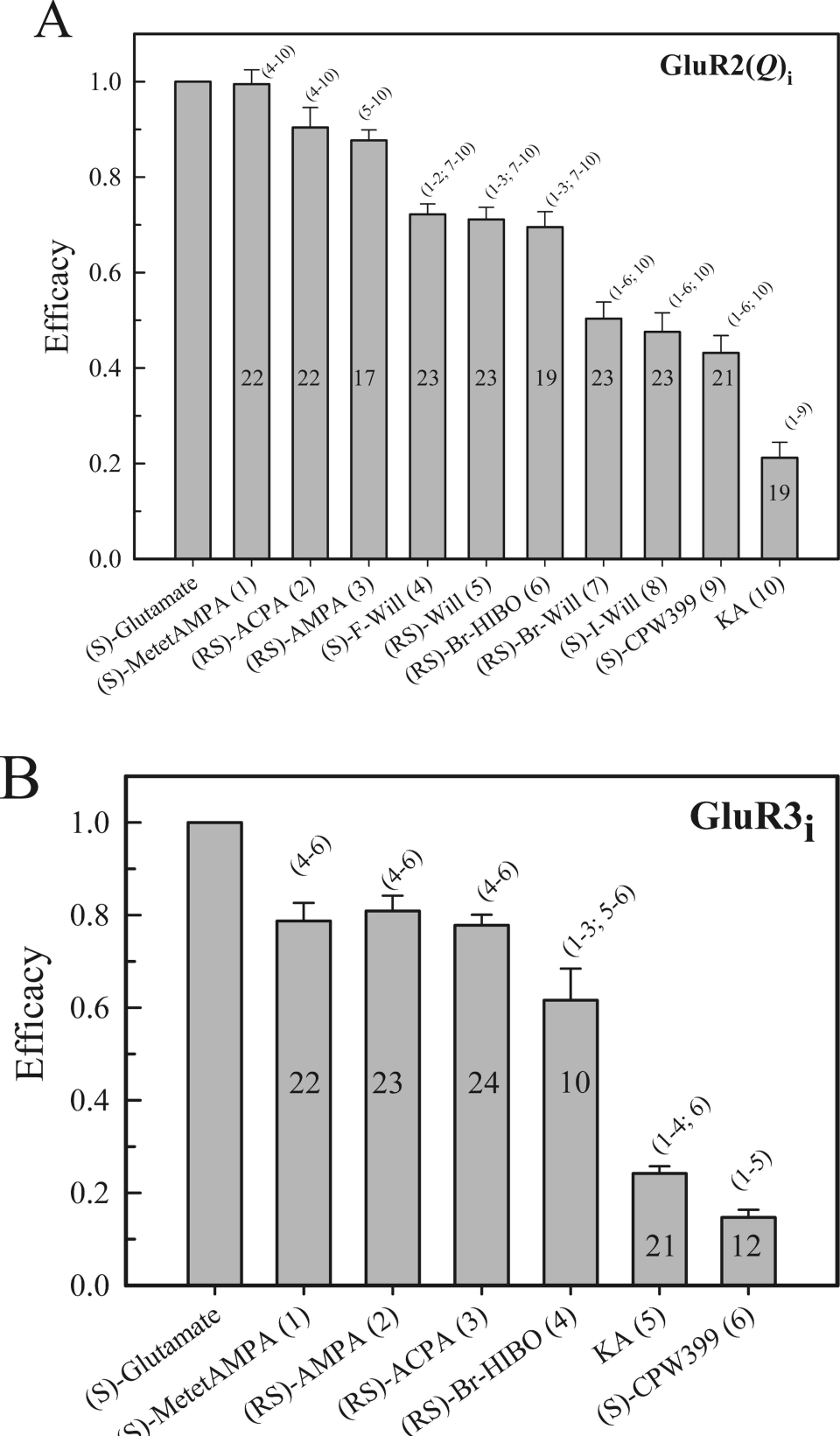
A
GluR2(Q)i
Efficacy
1.0
0.8
0.6
0.4
0.2
0.0
(4-10)
(4-10)
(5-10)
(1-2; 7-10)
(1-3; 7-10)
(1-3; 7-10)
(1-6; 10)
(1-6; 10)
(1-6; 10)
(1-9)
22
22
17
23
23
19
23
23
21
19
(S)-Glutamate
(S)-MetetAMPA (1)
(RS)-ACPA (2)
(RS)-AMPA (3)
(S)-F-Will (4)
(RS)-Will (5)
(RS)-Br-HIBO (6)
(RS)-Br-Will (7)
(S)-I-Will (8)
(S)-CPW399 (9)
KA (10)
B
GluR3i
Efficacy
1.0
0.8
0.6
0.4
0.2
0.0
(4-6)
(4-6)
(4-6)
(1-3; 5-6)
(1-4; 6)
(1-5)
22
23
24
10
21
12
(S)-Glutamate
(S)-MetetAMPA (1)
(RS)-AMPA (2)
(RS)-ACPA (3)
(RS)-Br-HIBO (4)
KA (5)
(S)-CPW399 (6)

Figure 4

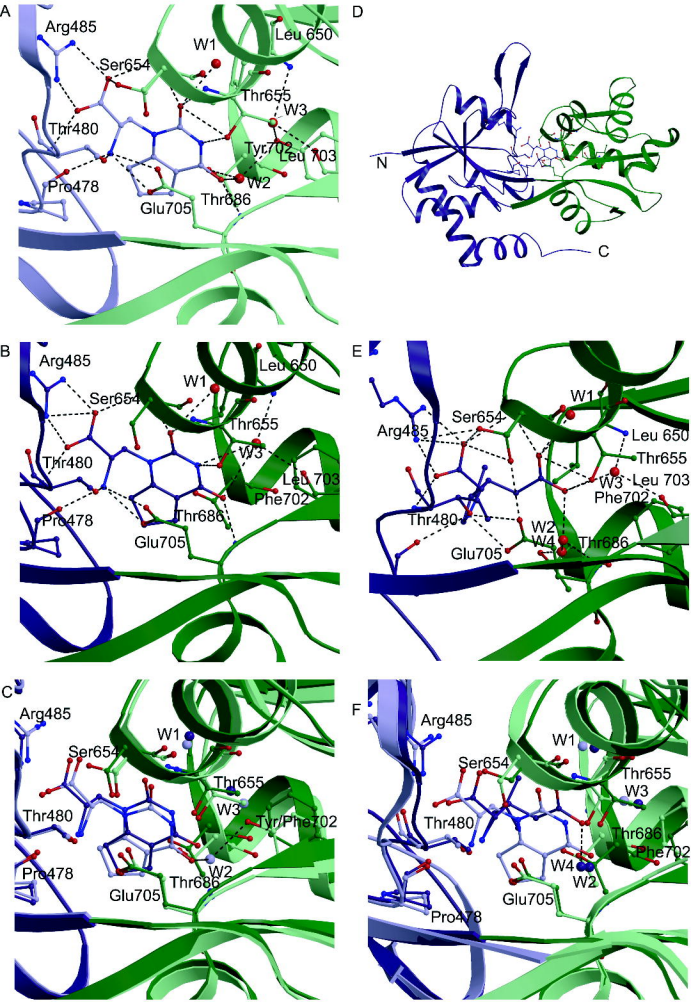
A
Arg485
Ser654
W1
Leu 650
Thr655
W3
Thr480
Tyr702
Leu 703
Pro478
W2
Glu705
Thr686
D
N
C
B
Arg485
Ser654
W1
Leu 650
Thr655
W3
Thr480
Leu 703
Phe702
Pro478
Thr686
Glu705
E
W1
Ser654
Arg485
Leu 650
Thr655
W3
Leu 703
Phe702
Thr480
W2
W4
Glu705
Thr686
C
Arg485
W1
Ser654
Thr655
W3
Thr480
Tyr/Phe702
Pro478
W2
Thr686
Glu705
F
Arg485
W1
Ser654
Thr655
W3
Thr480
Thr686
Phe702
W4
W2
Glu705
Pro478

Figure 5

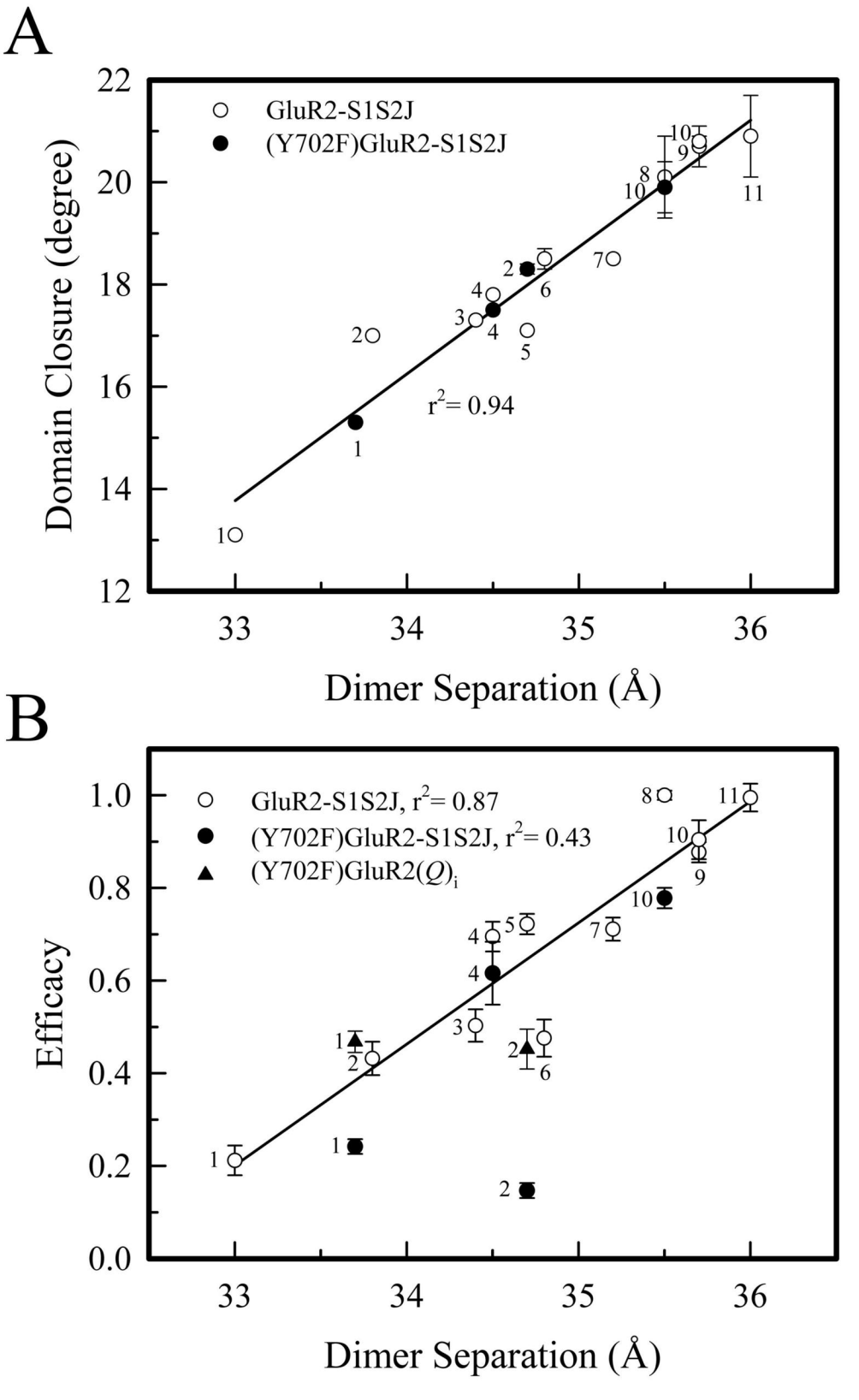
A
GluR2-S1S2J
(Y702F)GluR2-S1S2J
Domain Closure (degree)
Dimer Separation (Å)
r2= 0.94
B
GluR2-S1S2J, r2= 0.87
(Y702F)GluR2-S1S2J, r2= 0.43
(Y702F)GluR2(Q)i
Efficacy
Dimer Separation (Å)

Figure 6

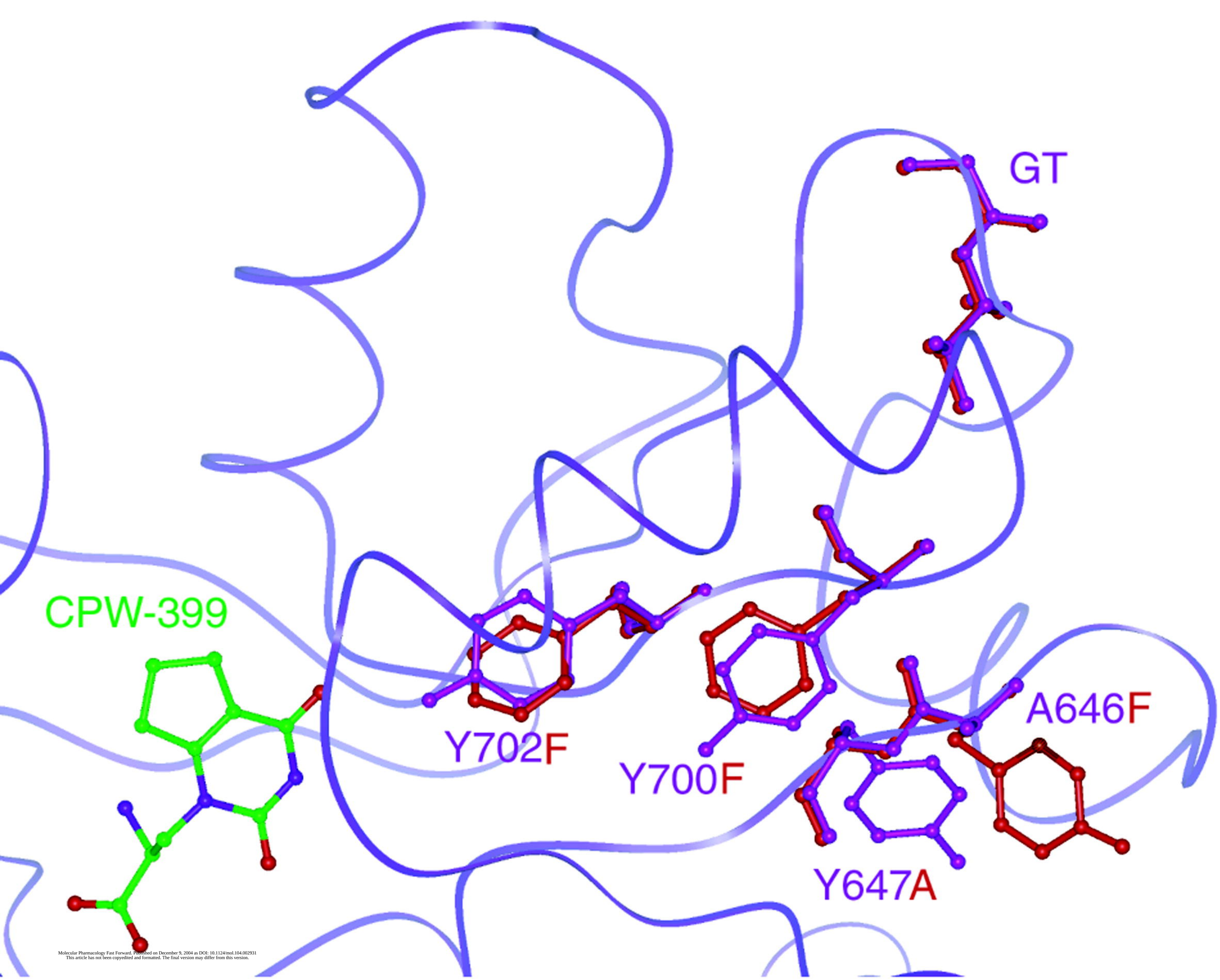

Figure 7